Eur Biophys J (2011) 40:775–782
DOI 10.1007/s00249-011-0691-6

ORIGINAL PAPER

Selectivity sequences in a model calcium channel: role of electrostatic field strength

Daniel Krauss · Bob Eisenberg · Dirk Gillespie

Received: 24 November 2010 / Revised: 2 February 2011 / Accepted: 16 February 2011 / Published online: 6 March 2011

Abstract The energetics that give rise to selectivity sequences of ionic binding selectivity of Li^+, Na^+, K^+, Rb^+, and Cs^+ in a model of a calcium channel are considered. This work generalizes Eisenman's classic treatment (Biophys J 2(Suppl. 2):259, 1962) by including multiple, mobile binding site oxygens that coordinate many permeating ions (all modeled as charged, hard spheres). The selectivity filter of the model calcium channel allows the carboxyl terminal groups of glutamate and aspartate side chains to directly interact with and coordinate the permeating ions. Ion dehydration effects are represented with a Born energy between the dielectric coefficients of the selectivity filter and the bath. High oxygen concentration creates a high field strength site that prefers small ions, as in Eisenman's model. On the other hand, a low filter dielectric constant also creates a high field strength site, but this site prefers large ions, contrary to Eisenman's model. These results indicate that field strength does not have a unique effect on ionic binding selectivity sequences once entropic, electrostatic, and dehydration forces are included in the model. Thus, Eisenman's classic relationship between field strength and selectivity sequences must be supplemented with additional information about selectivity filters such as the calcium channel that has amino acid side chains mixing with ions to make a crowded permeation pathway.

D. Krauss · B. Eisenberg · D. Gillespie (✉)
Department of Molecular Biophysics and Physiology,
Rush University Medical Center, Chicago, IL, USA
e-mail: dirk_gillespie@rush.edu

D. Krauss
Grinnell College, Grinnell, IA, USA

Keywords Eisenman selectivity sequences · Calcium channels · Selectivity · Modeling

Introduction

If Li^+, Na^+, K^+, Rb^+, and Cs^+ are placed in equimolar amounts outside a channel and allowed to permeate, only 11 of the 120 different possible sequences of binding selectivity have been found in actual channels. Eisenman described these selectivity sequences of ion binding in ion channels solely as a function of electrostatics and dehydration (Eisenman 1962; Eisenman and Horn 1983). His first model (Eisenman 1962) ignored many physical properties including entropy that are critical to accurately describe condensed matter systems such as an electrolyte in a channel. Despite its simplicity, Eisenman's model has proven to be remarkably accurate at predicting the 11 sequences that occur.

Here we expand on Eisenman's idea. In an early paper he noted that "While it is possible to extend the above calculations [for electrochemical potential] to assess the role of adjacent oxygens, silicons, and "screening" cations, the lack of detailed knowledge of their positions makes it more profitable at present to simplify the above representations by a single charged monopolar site" (Eisenman 1962). In our paper we include these adjacent oxygens and screening charges by modeling the oxygens as half-charged, mobile spheres that can coordinate the permeating ions. We also include a dielectric constant for the binding site to describe ion dehydration. Overall, this allows us to include electrostatics, dehydration, and entropic forces in our characterization of selectivity sequences in calcium channels, the main class of channels to which our model applies. While Eisenman and Alvarez (1991) have studied

the effect of nearby channel atoms in some specific channel structures, our approach allows us to *systematically* explore all possible outcomes (within the confines of our reduced model) in a system in which all atoms are at their free energy minimum. This approach then gives a broad brushstroke picture of selectivity sequences in calcium channels.

We observe that the two parameters within our model, the oxygen concentration and the filter dielectric constant, predict a wide range of selectivity sequences. Each parameter can increase the filter field strength, either by increasing oxygen concentration or by decreasing the filter dielectric constant. The oxygen concentration creates a typical correlation between the Eisenman sequences and "field strength." However, the dielectric constant of the filter results in a "high field strength" site that produces a "low field strength" selectivity sequence. Therefore, we conclude that selectivity in a model of a pore crowded with amino acids side chains cannot be characterized by one parameter such as field strength. Since ours is a very simple model, we speculate that the same is true in a real channel, a much more complicated system.

The Eisenman model

In this section we will give a brief review of the basic Eisenman model (1962), ignoring its many generalizations and extensions [see Eisenman and Horn (1983) and references therein]. Eisenman modeled the alkali ions as equivalent charged spheres with their Goldschmidt radii and the binding site as a sphere with a charge of -1. This model is based on the physics of ion-selective glass electrodes. By simple electrostatic calculations, one can compute the energy of the system to show that the smaller the ion, the higher its affinity for a sphere of that diameter (Eisenman 1962; Hille 2001).

With just this information, the only selectivity sequence that could be observed would be $Li^+ > Na^+ > K^+ > Rb^+ > Cs^+$ (sequence XI; Table 1). The smaller ion will always be able to move closer to the binding site charge. However, if ions dehydrate before they permeate, Eisenman sequences come from the competition between binding and dehydration, and one can observe a myriad of selectivity sequences. As the size of the binding site sphere changes from small to large, the Eisenman selectivity sequences are observed (Table 1). Eisenman defined a sequence corresponding to a small sphere as a "high field strength" site and those corresponding to a large sphere as "low field strength." He could then apply "field strength" to actual channels based on their selectivity properties.

The Eisenman sequences are then the result of two competing phenomena, the attraction of the ion into the charged binding site and the dehydration penalty for entering the binding site. Generalizing the work of Krasne and Eisenman (1973), Eisenman and Horn (1983) showed that the sequences arise as long as the attraction term falls off as a function of ion size as a lower power than the dehydration term. While this approach is simple in principle, some have criticized this "field strength" argument. Armstrong (1989), for example, demonstrated that the Eisenman procedure is very inaccurate when predicting relative ratios between ions. He also showed that the sequences observed are very sensitive to the particular diameter used. If, for instance, Pauling radii are used in the place of Goldschmidt radii, no K^+ selective channels are observed. This makes it possible that the 11 Eisenman sequences do not correspond to Eisenman's "field strength."

Table 1 List of all selectivity sequences observed in Fig. 1 with their percentage of the total

Eisenman sequences			Non-Eisenman sequences		
Seq. no.	Sequence	Percentage of total	Seq. no.	Sequence	Percentage of total
I	$Cs^+ > Rb^+ > K^+ > Na^+ > Li^+$	9.29	i	$Rb^+ > Na^+ > K^+ > Li^+ > Cs^+$	0.002
II	$Rb^+ > Cs^+ > K^+ > Na^+ > Li^+$	5.64	ii	$Rb^+ > Na^+ > K^+ > Cs^+ > Li^+$	1.16
III	$Rb^+ > K^+ > Cs^+ > Na^+ > Li^+$	3.02	iii	$Rb^+ > Na^+ > Cs^+ > K^+ > Li^+$	0.006
IV	$K^+ > Rb^+ > Cs^+ > Na^+ > Li^+$	0	iv	$Rb^+ > K^+ > Na^+ > Cs^+ > Li^+$	2.70
V	$K^+ > Rb^+ > Na^+ > Cs^+ > Li^+$	0	v	$Rb^+ > Cs^+ > Na^+ > K^+ > Li^+$	0.003
VI	$K^+ > Na^+ > Rb^+ > Cs^+ > Li^+$	0	vi	$Na^+ > Rb^+ > Li^+ > K^+ > Cs^+$	0.14
VII	$Na^+ > K^+ > Rb^+ > Cs^+ > Li^+$	0.71	vii	$Na^+ > Rb^+ > K^+ > Li^+ > Cs^+$	1.01
VIII	$Na^+ > K^+ > Rb^+ > Li^+ > Cs^+$	2.76	viii	$Na^+ > Rb^+ > K^+ > Cs^+ > Li^+$	1.73
IX	$Na^+ > K^+ > Li^+ > Rb^+ > Cs^+$	0.59	ix	$Na^+ > Li^+ > Rb^+ > K^+ > Cs^+$	0.63
X	$Na^+ > Li^+ > K^+ > Rb^+ > Cs^+$	8.17	x	$Li^+ > Na^+ > Rb^+ > K^+ > Cs^+$	1.04
XI	$Li^+ > Na^+ > K^+ > Rb^+ > Cs^+$	61.40			
Total		91.6	Total		8.4

As an alternative, Armstrong suggested that any theory that produced a single peak when affinity is plotted as a function of permeant ion radius will produce the Eisenman sequences (plus five others) (Armstrong 1989). The balance of electrostatic attraction and ion dehydration does this since each energy is monotonic in ion radius (but of opposite sign). Later we show that Armstrong's idea does not hold in our model when the filter dielectric constant is very low.

Reduced calcium channel model

Our model is an extension of Eisenman's original work (Eisenman 1962). Selectivity within our model is fundamentally based on a balance of dehydration and electrostatics, just like within his model. Eisenman made clear that he wanted to push his model further to include the roles of multiple pore charges and screening cations, but lacked the structural data, ionic theory, and computational power to do so.

Our reduced model of a calcium channel consists of two bulk fluids (homogeneous and infinite in all directions) consisting of ions modeled as charged hard spheres. Water is implicitly present in each compartment as dielectric constants, one for each fluid. One fluid represents the bath outside the channel and contains the permeating ions. The other fluid represents the selectivity filter and contains a given concentration of half-charged oxygen ions ($O^{1/2-}$). These oxygens represent the carboxyl oxygens present in the selectivity filter of calcium channels or the carbonyl oxygens of the protein backbone of K^+ channels. Koch et al. (2000) have shown that the glutamates of L-type calcium channels face the permeation pathway and therefore can directly interact with the permeating ions.

The oxygens are modeled as a fluid so that they can coordinate the permeating ions, which has been shown to give calcium channels their selectivity (Boda et al. 2000, 2002; Gillespie 2008; Nonner et al. 2000). Because the fluid is infinite in all directions, the model makes no distinction between having n oxygens in a filter of volume v and having αn oxygens in a filter of volume αv. Thus, any channel geometry is represented through $[O^{1/2-}]$; the selectivity filter does not have an explicit length or radius.

$[O^{1/2-}]$ also determines selectivity. As an example, $[O^{1/2-}] = 40$ M behaves somewhat like the highly Ca^{2+} selective L-type Ca^{2+} channel while $[O^{1/2-}] = 20$ M behaves more like the mildly Ca^{2+} selective ryanodine receptor calcium channel (Krauss and Gillespie 2010; Nonner et al. 2000). Theoretical studies support the assumption that oxygen concentration as opposed to size or shape of the filter determines the number of ions that move into the filter (Malasics et al. 2009). By changing the oxygen concentration, we alter the charge density of the filter. A higher $[O^{1/2-}]$ therefore results in a higher field strength site.

The dielectric constant within the filter gives us a way of including water and dehydration (Nonner et al. 2001). If the dielectric constant within the filter is the same as the bath (78.4), all waters of hydration are free to move into the channel, and there are zero penalties for shedding waters of hydration. On the other hand, if the channel's dielectric constant is lower than that of the bath, the channel can better exclude waters of hydration and thus has penalties for shedding waters of hydration. Reducing the filter's dielectric constant also reduces the amount of water between the screening charge and therefore also increases the interactions between the ions and between the ions and the oxygens. This means that a low dielectric constant results in a high field strength site.

While this model is greatly simplified, it has the key selectivity properties of calcium channels (Nonner et al. 2000). This model is by no means quantitatively accurate. However, many studies have shown that, in calcium channels, selectivity is determined primarily by a balance of cations entering the filter to screen the negative amino acids and a lack of space in the crowded filter, exactly the two forces that act on the system within our model (Boda et al. 2000, 2001, 2002, 2006 2007, 2008, 2009; Gillespie 2008; Gillespie and Boda 2008; Gillespie et al. 2005, 2008, 2009; Gillespie and Fill 2008; Malasics et al. 2009; Miedema et al. 2004, 2006; Nonner et al. 2000, 2001 Nonner and Eisenberg 1998; Rodriguez-Contreras et al. 2002). This reduced model of amino acids in the selectivity filter has successfully modeled calcium selectivity in the pores such as the L-type calcium channel and the ryanodine receptor. It has also reproduced and predicted experimental data in many cases (Boda et al. 2009; Gillespie 2008; Gillespie and Boda 2008; Gillespie and Fill 2008; Gillespie et al. 2005, 2009; Miedema et al. 2004, 2006; Nonner et al. 2000; Rodriguez-Contreras et al. 2002).

The system in this paper uses the mean spherical approximation (MSA) to compute the electrochemical potential of these ions (Barthel et al. 1998; Blum 1975, 1980; Nonner et al. 2000; 2001; Waisman and Lebowitz 1970). Given the bath concentrations, valences, and ionic radii of all the permeating ions and the concentration of oxygens in the filter, we can use the MSA theory for the excess chemical potential to determine the concentration of each bath ion in the filter. Since our system is in equilibrium, the chemical potential for all ions is the same for the bath and the filter so that, for ion species X,

$$\mu_X^{bath} = \overbrace{kT \cdot \ln\left(\Lambda_X^3 [X]_{filter}\right)}^{\text{ideal gas}} + \overbrace{z_X V_D}^{\text{mean electrostatic}} + \overbrace{\mu_X^{SC}}^{\text{screening}} + \overbrace{\mu_X^{HS}}^{\text{excluded volume}} + \overbrace{\mu_X^{dehydr} \frac{\varepsilon_{filter} - \varepsilon_{bath}}{\varepsilon_{filter}(\varepsilon_{bath} - 1)}}^{\text{dehydration}} \quad (1)$$

where μ_X^{bath} is the electrochemical potential of the ion in the bath, k is the Boltzmann constant, T is temperature in Kelvin, $[X]_{filter}$ is concentration of the ion in the filter, z_X is valence, V_D is Donnan (electrical) potential, μ_X^{SC} is the term representing the ion screening the charges around it, μ_X^{HS} is the excluded volume term, μ_X^{dehydr} is the ion's Gibbs free energy of hydration (Table 2), ε_{filter} is the filter dielectric constant, and ε_{bath} is the bath dielectric constant.

The excess chemical potential contains four terms in this model. An excluded volume portion (μ_X^{HS}) represents the chemical potential created by volume exclusion (i.e., two hard sphere ions cannot overlap). The electrostatic portion contains two parts, a mean electrostatic potential (V_D) and a screening component (μ_X^{SC}). The former is the long-time, many-particle average of the electrostatic potential, while the latter describes the energy of ions rearranging to screen each other, with small ions lowering the free energy of the system because they screen better than larger ions that cannot approach as closely (Gillespie 2008). The dehydration term is represented as a Born scaling of the experimental Gibbs free energy of hydration with a dielectric constant, as was done previously by Nonner et al. (2001).

For the bath, we have the concentrations of all ions within the system, and we set the mean electrostatic potential to 0. This allows us to define the chemical potential for the bath μ_X^{bath} from the concentrations of the permeating ions. For the filter, however, we only know the concentration of the oxygens, but we do not know the chemical potential of the oxygens because we do not know the final concentrations of permeant ions in the filter. This can be overcome by including the Donnan potential for the filter since solving for V_D implicitly defines the oxygens' chemical potential. To find V_D, we assume charge neutrality in the filter because it is a bulk fluid. The Donnan potential is almost never 0 and can, under some circumstances, be quite large (e.g., when the permeant ions have large deydration penalties). We can then numerically solve for the unknowns using Mathematica (version 7, Wolfram Research, Champaign, IL) to determine ionic concentrations in the filter and, thus, selectivity.

Table 2 Properties of all ions present in the system

Ion	Diameter (Å)	μ_X^{dehydr} (kJ/mol)
Li^+	1.33	−529.4
Na^+	2.00	−423.7
K^+	2.76	−351.9
Rb^+	2.98	−329.3
Cs^+	3.40	−306.1
Cl^-	3.62	−304.0
$O^{1/2-}$	2.80	–

Ion diameters are crystal diameters from Shannon and Prewitt (1969) and the experimental Gibbs free energies of hydration are from Fawcett (1999)

Results

We considered selectivity of channels with filter ε_{filter} ranging from 3 to 80 and oxygen concentration ranging from 1 to 25 M with Li^+, Na^+, K^+, Rb^+, and Cs^+ present in the bath at 50 mM. To the bath, 250 mM Cl^- was added to balance out the charge from the cations. For each channel, we determined the selectivity sequence of the five cations by computing the concentration of each ion species in the filter. The sequences observed, listed in Table 1, occurred in distinct regions as shown in Fig. 1. Eight of the 11 Eisenman sequences were observed, and 10 non-Eisenman sequences were observed (lowercase Roman numerals in Fig. 1). Selectivity trended towards large ions at low dielectrics and low oxygen concentrations.

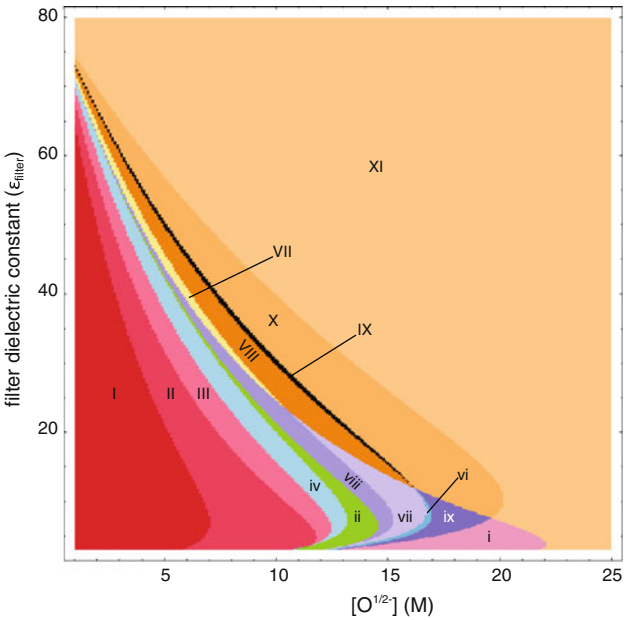

Fig. 1 Monovalent cation selectivity sequences for all channels with $[O^{1/2-}] = 1$–25 M and $\varepsilon_{filter} = 3$–80. The five cations were each present at 50 mM in the bath along with 250 mM Cl^-. *Roman numerals* correspond to the selectivity sequences listed in Table 1. *Uppercase numerals* denote Eisenman sequences and *lowercase* non-Eisenman sequences

At high filter dielectric constants (≥ 75), the oxygen concentration had no effect on selectivity. However, at lower dielectrics increasing the oxygen concentration caused a trend towards small ion selectivity (while keeping $\varepsilon_{\text{filter}}$ fixed). This trend generally followed the Eisenman sequences from I to XI with a few non-Eisenman sequences in a discrete band in the middle of our data range. The higher oxygen concentration increased the weight of the hard sphere and electrostatic terms in the chemical potential (Eq. 1). The hard sphere portion increased as oxygen concentration rose until volume exclusion became the dominant factor in determining selectivity (Fig. 2). This figure shows, as a function of oxygen concentration, the binding selectivity between K^+ and Na^+ which was defined by Gillespie (2008):

$$\overbrace{\ln\left(\frac{[K^+]_{\text{filter}}}{[Na^+]_{\text{filter}}}\right)}^{\text{binding selectivity}} = \overbrace{\ln\left(\frac{[K^+]_{\text{bath}}}{[Na^+]_{\text{bath}}}\right)}^{\text{number advantage}} + \overbrace{\frac{1}{kT}\left(\Delta\mu_K^{SC} - \Delta\mu_{Na}^{SC}\right)}^{\text{screening advantage}} + \overbrace{\frac{1}{kT}\left(\Delta\mu_K^{HS} - \Delta\mu_{Na}^{HS}\right)}^{\text{excluded volume advantage}} + \overbrace{(\mu_K^{\text{dehydr}} - \mu_{Na}^{\text{dehydr}})\frac{\varepsilon_{\text{filter}} - \varepsilon_{\text{bath}}}{\varepsilon_{\text{filter}}(\varepsilon_{\text{bath}} - 1)}}^{\text{dehydration advantage}} \quad (2)$$

where the Δ indicates the difference between the filter and bath values of that component of the chemical potential of ion X. A positive term in Eq. 2 favors K^+ binding in the filter while a negative one favors Na^+.

The figure shows each component of the binding selectivity of Eq. 2. The dehydration term remains relatively constant and in favor of K^+ since the filter dielectric constant does not change (from 50) during these calculations. As oxygen concentration increases, the hard sphere term becomes larger and eventually increases to over four times the dehydration energy. Since the entropic effect is so large, it is the main determinant of the selectivity of the system in this region of the parameter space.

Changes to the dielectric constant of the filter produce a similar trend with large dielectrics resulting in small ion selectivity (Fig. 3). Much like in Fig. 2, this figure presents the difference in chemical potential and its components of Eq. 2, this time as a function of dielectric constant in the filter. When the filter dielectric approaches that of the bath (78.4), the dehydration penalties and the electrostatic interaction both approach 0. This means that the excluded volume term becomes the largest determinant of electrochemical potential and thus selectivity in the high $\varepsilon_{\text{filter}}$ regime.

For small filter dielectrics, the picture gets a bit murkier. The screening component of the chemical potential and dehydration both become very large and are of opposite signs, yet the difference between the two is still relatively small. Therefore, small changes to how each term is computed have large effects on the selectivity sequence observed. In order to accurately predict sequences in this region, our model would need more detailed knowledge about the environment of the channel and more accurate theories of the ions and their dehydration. While probably inaccurate in this region, our model should produce the correct trend in selectivity for $\varepsilon_{\text{filter}} \geq 15$.

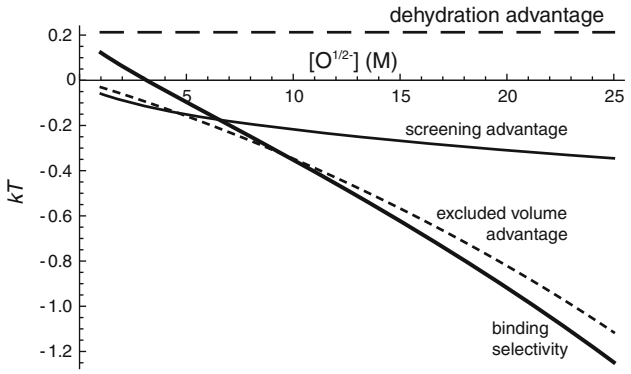

Fig. 2 Differences in the components of the electrochemical potential (Eq. 2) between K^+ and Na^+ as a function of $[O^{1/2-}]$. The *thin solid line* corresponds to the screening advantage, the *dotted line* to the hard sphere advantage, the *dashed line* to the dehydration advantage, and *the thick, solid line* to the total of the other *four lines*, the overall binding selectivity. *Positive values* indicate the term favors K^+ over Na^+ accumulating in the filter while *negative values* indicate the opposite selectivity. The mean electrostatic and ideal gas components are the same for both ions and are not included. In this figure, $\varepsilon_{\text{filter}} = 50$

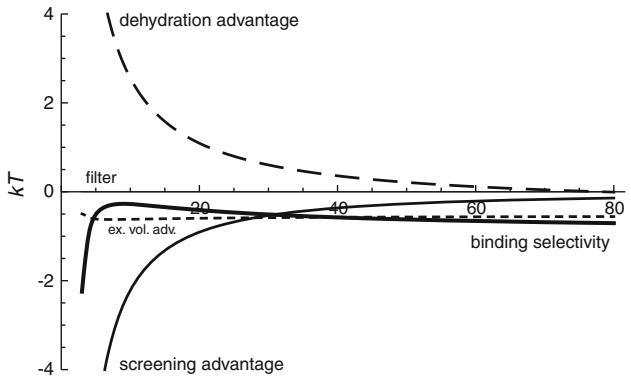

Fig. 3 Differences in the components of the electrochemical potential (Eq. 2) between K^+ and Na^+ as a function of $\varepsilon_{\text{filter}}$. The *thin solid line* corresponds to the screening advantage, the *dotted line* to the hard sphere advantage, the *dashed line* to the dehydration advantage, and *the thick, solid line* to the total of the other *four lines*, the overall binding selectivity. *Positive values* favor K^+ accumulating in the filter. The mean electrostatic and ideal gas components are the same for both ions and are not included. In this figure, $[O^{1/2-}] = 15$ M

While the vast majority of the selectivity sequences produced by the model are Eisenman sequences, we also calculated a band of other sequences (the collection of lowercase Roman numerals in Fig. 1). This band represents approximately 8.4% of channels with sequences that do not match any of the 11 standard Eisenman sequences (or even the extended 13 Eisenman sequences). They are broken down in a histogram in Fig. 4. Ten non-Eisenman sequences were observed, but only five represented more than 1% of the total sequences (Table 1). These 10 sequences were generally Rb^+ or Na^+ selective while 1 was Li^+ selective. Despite being non-Eisenman sequences, they appeared in a distinct band of oxygen concentrations and dielectrics (Fig. 1) and generally only had one pair of ions out of order when compared to an Eisenman sequence that existed near that band.

Discussion

We have shown that as we change the oxygen concentration and the dielectric constant of the filter within our model, we observe many of the 11 Eisenman sequences in order. As oxygen concentration increases, the sequences trend from I to XI (Table 1). As the dielectric constant increases the sequences trend from XI to I.

Our model provides two definitions for field strength that correspond to these parameters. A channel with a high oxygen concentration produces a "high field strength" sequence because it increases the number of charges within the filter. Because of the steric effects caused by the oxygens, a high $[O^{1/2-}]$ channel becomes small ion selective and produces a "high field strength" sequence.

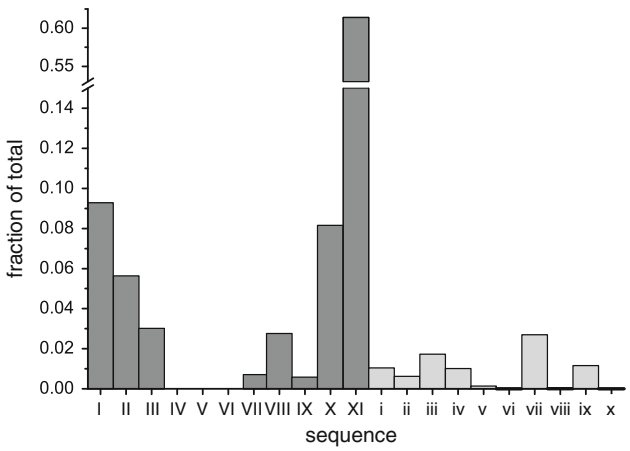

Fig. 4 Histogram of the data from Fig. 1. Each count is expressed as a percentage of the total number of sequences observed. *Roman numerals* correspond to the selectivity sequences in Table 1. *Dark gray columns* correspond to Eisenman sequences while *light gray columns* correspond to non-Eisenman sequences

A low $\varepsilon_{\text{filter}}$ means that water is excluded, increasing charge-charge interactions, and thereby increasing field strength. However, we find that a high $\varepsilon_{\text{filter}}$ produces an Eisenman "high field strength" sequence. When the dehydration penalty is negligible ($\varepsilon_{\text{filter}} \geq 70$), the channel is selective for small ions at virtually all oxygen concentrations. This appears to contradict Eisenman's definition of electrostatic field strength because a "high field strength" selectivity sequence should imply increased charge-charge interaction. Increased charge-charge interactions actually occur at low $\varepsilon_{\text{filter}}$ instead of at high $\varepsilon_{\text{filter}}$ in our calculations, the opposite of what would be classically expected.

In Eisenman's work the binding site charges were fixed in place because the binding site was a glass (Eisenman 1962). However, calcium channels have mobile binding site charges. This allows for some waters to enter. The filter dielectric constant this produces couples "field strength" and the dehydration penalty. The field strength can be decreased by having more waters around the screening charges. This extra water decreases charge-charge interactions while simultaneously decreasing the magnitude of dehydration penalties. In Eisenman's calculations, the number of waters admitted into the channel did not affect selectivity. This is because without an entropic term, the magnitude of the dehydration penalties would have to become much smaller than we calculate before they would affect selectivity.

In the Eisenman model of a glass electrode, a single particle moving to a single binding site has no entropic effect; the screening charge does not have to fit between other screening ions and compete for space. However, this model of rigid glass electrodes may not be a good representation of a calcium channel that has amino acid side chains crowding the permeation pathway. In our model, the excluded volume term is relatively constant as a function of $\varepsilon_{\text{filter}}$ in our chemical potential calculations (Fig. 3). Therefore, at high dielectric constants the relative differences between the dehydration penalties would not alter selectivity because the hard sphere term is so much larger than the dehydration penalties. Once entropic effects are included and charge-charge interaction is coupled with dehydration energy through a dielectric constant, we observe large ion selectivity in certain "high field strength" sites (Fig. 3).

While "field strength" may not work as a determinant of selectivity, our calculations generally support the monotonic viewpoint of Armstrong (1989) when $\varepsilon_{\text{filter}} > 15$. Only a single peak in an affinity (ion concentrations in the filter) as a function of ionic diameter is observed for all of the channels with Eisenman sequences, which were 91% of the observed sequences. However, among the non-Eisenman sequences we computed, only 1 of the 10, namely

$Rb^+ > K^+ > Na^+ > Cs^+ > Li^+$ (iv), followed Armstrong's argument. The other nine non-Eisenman sequences depart from Armstrong's argument and occurred mostly at very low ($\varepsilon_{filter} \leq 15$) filter dielectric constants (Fig. 1). In fact, at extremely low filter dielectric constant ($\varepsilon_{filter} \leq 8$) we found multiple peaks when affinity is plotted versus ionic radius (data not shown). However, below $\varepsilon_{filter} = 15$ our model is probably quite inaccurate because of the very large attractive Coulombic forces and the very large repulsive dehydration penalties (Fig. 3). The balance of these two large forces will always be hard to calculate, and our simple model is no exception.

This parameter space region of low filter dielectric constant is also interesting because these parameters characterize potassium channels. Potassium channels can generally be described as excluding almost all waters and as having a large dipole and oxygen density (Doyle et al. 1998). This describes exactly the lower region of Fig. 1 in which most of these sequences occur. Our data show K^+ versus Na^+ selectivity only in essentially gaseous environments (very low oxygen concentration and ε_{filter}), which is consistent with gas-phase experiments of ion binding with water molecules (Dzidic and Kebarle 1970). This seems to contradict the idea that potassium channels have large oxygen concentrations and low dielectric constants. However, theoretical studies on potassium channels show that the key difference between our high oxygen/low dielectric channels and a potassium channel is the lack of constraint on oxygen movement in our model; in the potassium channel the oxygens cannot move to fully coordinate the permeating ions. A potassium channel's filter charges are not present in the permeation pathway as in our model, and they do not move very freely as we allow our oxygens to do (Fowler et al. 2008). This constraint on the oxygens' ability to fully coordinate the permeating ions produces K^+ selectivity over Na^+. This supports the argument that constraints on the oxygens' freedom of movement produces K^+ selectivity (Bostick and Brooks 2007; Thomas et al. 2007; Varma and Rempe 2007; Varma et al. 2008).

Conclusion

Our reduced model of a calcium channel produces 8 of the 11 Eisenman sequences, showing that the basic results of Eisenman continue to have staying power. The non-Eisenman sequences we found were only 8.4% of the sequences we calculated. However, contrary to Eisenman's classic mechanism for these selectivity sequences, we found that in a model with entropic, electrostatic, and dehydration components, electrostatic field strength does not relate directly and monotonically to selectivity sequences. Specifically, two different model parameters could be used to define a high field strength binding site, but they produced exactly opposite selectivity sequences (I and XI). Since a real channel is much more complex than our model, we conclude that the field strength characterizations probably do not hold in real channels as well.

Acknowledgments D.G. and D.K. were supported by NIH grant R01-AR054098. B.E. was supported in part by NIH grant GM076013. We thank Sameer Varma for very useful discussions about potassium channels and how they relate to our work.

References

Armstrong CM (1989) Reflections on selectivity. In: Tosteson DC (ed) Membrane transport: people and ideas. American Physiological Society, Bethesda, pp 261–273

Barthel JMG, Krienke H, Kunz W (1998) Physical chemistry of electrolyte solutions: modern aspects. Springer, New York

Blum L (1975) Mean spherical model for asymmetric electrolytes I: method of solution. Mol Phys 30:1529–1535

Blum L (1980) Solution of the Ornstein-Zernike equation for a mixture of hard ions and Yukawa closure. J Stat Phys 22:661–672

Boda D, Busath DD, Henderson D, Sokołowski S (2000) Monte Carlo simulations of the mechanism of channel selectivity: the competition between volume exclusion and charge neutrality. J Phys Chem B 104:8903–8910

Boda D, Henderson D, Busath DD (2001) Monte Carlo study of the effect of ion and channel size on the selectivity of a model calcium channel. J Phys Chem B 105:11574–11577

Boda D, Henderson D, Busath DD (2002) Monte Carlo study of the selectivity of calcium channels: improved geometry. Mol Phys 100:2361–2368

Boda D, Valiskó M, Eisenberg B, Nonner W, Henderson D, Gillespie D (2006) The effect of protein dielectric coefficient on the ionic selectivity of a calcium channel. J Chem Phys 125:034901

Boda D, Valiskó M, Eisenberg B, Nonner W, Henderson D, Gillespie D (2007) Combined effect of pore radius and protein dielectric coefficient on the selectivity of a calcium channel. Phys Rev Lett 98:168102

Boda D, Nonner W, Henderson D, Eisenberg B, Gillespie D (2008) Volume exclusion in calcium selective channels. Biophys J 94:3486–3496

Boda D, Valiskó M, Henderson D, Eisenberg B, Gillespie D, Nonner W (2009) Ionic selectivity in L-type calcium channels by electrostatics and hard-core repulsion. J Gen Physiol 133:497–509

Bostick D, Brooks CL III (2007) Selectivity in K^+ channels is due to topological control of the permeant ion's coordinated state. Proc Natl Acad Sci USA 104:9260–9265

Doyle DA, Morais Cabral J, Pfuetzner RA, Kuo A, Gulbis JM, Cohen SL, Chait BT, MacKinnon R (1998) The structure of the potassium channel: molecular basis of K^+ conduction and selectivity. Science 280:69–77

Dzidic I, Kebarle P (1970) Hydration of the alkali ions in the gas phase: enthalpies and entropies of reactions $M + (H2O)_{n-1} + H2O = M + (H2O)_n$. J Phys Chem 74:1466–1474

Eisenman G (1962) Cation selective glass electrodes and their mode of operation. Biophys J 2(Suppl. 2):259–323

Eisenman G, Alvarez O (1991) Structure and function of channels and channelogs as studied by computational chemistry. J Membr Biol 119:109–132

Eisenman G, Horn R (1983) Ionic selectivity revisited: the role of kinetic and equlibrium processes in ion permeation through channels. J Membr Biol 76:197–225

Fawcett WR (1999) Thermodynamic parameters for the solvation of monatomic ions in water. J Phys Chem B 103:11181–11185

Fowler PW, Tai K, Sansom MSP (2008) The selectivity of K^+ ion channels: testing the hypotheses. Biophys J 95:5062–5072

Gillespie D (2008) Energetics of divalent selectivity in a calcium channel: the ryanodine receptor case study. Biophys J 94:1169–1184

Gillespie D, Boda D (2008) The anomalous mole fraction effect in calcium channels: a measure of preferential selectivity. Biophys J 95:2658–2672

Gillespie D, Fill M (2008) Intracellular calcium release channels mediate their own countercurrent: the ryanodine receptor case study. Biophys J 95:3706–3714

Gillespie D, Xu L, Wang Y, Meissner G (2005) (De)constructing the ryanodine receptor: modeling ion permeation and selectivity of the calcium release channel. J Phys Chem B 109:15598–15610

Gillespie D, Boda D, He Y, Apel P, Siwy ZS (2008) Synthetic nanopores as a test case for ion channel theories: the anomalous mole fraction effect without single filing. Biophys J 95:609–619

Gillespie D, Giri J, Fill M (2009) Reinterpreting the anomalous mole fraction effect: the ryanodine receptor case study. Biophys J 97:2212–2221

Hille B (2001) Ion channels of excitable membranes, 3rd edn. Sinauer Associates, Sunderland

Koch SE, Bodi I, Schwartz A, Varadi G (2000) Architecture of Ca^{2+} channel pore-lining segments revealed by covalent modification of substituted cysteines. J Biol Chem 275:34493–34500

Krasne S, Eisenman G (1973) The molecular basis of ion selectivity. In: Eisenman G (ed) Membranes: a series of advances: lipid bilayers and antibiotics, vol 2. Marcel Dekker, New York

Krauss D, Gillespie D (2010) Sieving experiments and pore diameter: it's not a simple relationship. Eur Biophys J 39:1513–1521

Malasics A, Gillespie D, Nonner W, Henderson D, Eisenberg B, Boda D (2009) Protein structure and ionic selectivity in calcium channels: selectivity filter size, not shape, matters. Biochim Biophys Acta Biomembr 1788:2471–2480

Miedema H, Meter-Arkema A, Wierenga J, Tang J, Eisenberg B, Nonner W, Hektor H, Gillespie D, Meijberg W (2004) Permeation properties of an engineered bacterial OmpF porin containing the EEEE-locus of Ca^{2+} channels. Biophys J 87:3137–3147

Miedema H, Vrouenraets M, Wierenga J, Gillespie D, Eisenberg B, Meijberg W, Nonner W (2006) Ca^{2+} selectivity of a chemically modified OmpF with reduced pore volume. Biophys J 91:4392–4400

Nonner W, Eisenberg B (1998) Ion permeation and glutamate residues linked by Poisson-Nernst-Planck theory in L-type calcium channels. Biophys J 75:1287–1305

Nonner W, Catacuzzeno L, Eisenberg B (2000) Binding and selectivity in L-type calcium channels: a mean spherical approximation. Biophys J 79:1976–1992

Nonner W, Gillespie D, Henderson D, Eisenberg B (2001) Ion accumulation in a biological calcium channel: effects of solvent and confining pressure. J Phys Chem B 105:6427–6436

Rodriguez-Contreras A, Nonner W, Yamoah EN (2002) Ca^{2+} transport properties and determinants of anomalous mole fraction effects of single voltage-gated Ca^{2+} channels in hair cells from bullfrog saccule. J Physiol 538:729–745

Shannon RD, Prewitt CT (1969) Effective ionic radii in oxides and fluorides. Acta Crystallogr B25:925–946

Thomas M, Jayatilaka D, Corry B (2007) The predominant role of coordination number in potassium channel selectivity. Biophys J 93:2635–2643

Varma S, Rempe S (2007) Tuning ion coordination architectures to enable selective partitioning. Biophys J 93:1093–1099

Varma S, Sabo D, Rempe SB (2008) K^+/Na^+ selectivity in K channels and valinomycin: over-coordination versus cavity-size constraints. J Mol Biol 376:13–22

Waisman E, Lebowitz JL (1970) Exact solution of an integral equation for the structure of a primitive model of an electrolyte. J Chem Phys 52:4307–4309